HOKKAIDO UNIVERSITY

Title	Design of PLC E31-E13 and E-LP tapered mode converters using fast quasiadiabatic dynamics
Author(s)	Wang, Han; Fujisawa, Takeshi; Sato, Takanori; Wada, Masaki; Mori, Takayoshi; Sakamoto, Taiji; Imada, Ryota; Matsui, Takashi; Nakajima, Kazuhide; Saitoh, Kunimasa
Citation	IEICE electronics express, 20230392 https://doi.org/10.1587/elex.20.20230392
Issue Date	2023-12-10
Doc URL	http://hdl.handle.net/2115/90935
Rights	Copyright ©2023 The Institute of Electronics, Information and Communication Engineers
Type	article
File Information	20_20.20230392.pdf

Instructions for use

Hokkaido University Collection of Scholarly and Academic Papers : HUSCAP

IEICE Electronics Express, Vol.20, No.23, 1–6

LETTER

Design of PLC E_{31}-E_{13} and E-LP tapered mode converters using fast quasiadiabatic dynamics

Han Wang[1, a)], Takeshi Fujisawa[1], Takanori Sato[1], Masaki Wada[2], Takayoshi Mori[2], Taiji Sakamoto[2], Ryota Imada[2], Takashi Matsui[2], Kazuhide Nakajima[2], and Kunimasa Saitoh[1]

Abstract The previous PLC E_{31} and E_{13} mode converters employ linear tapered structures to fulfill the adiabatic coupling condition and achieve a high mode conversion efficiency, which requires long taper lengths. In this paper, we propose two types of PLC tapered structures that can be applied in different scenarios using fast quasiadiabatic dynamics. These structures enable mode conversions of E_{31}-E_{13} modes, as well as E_{31}-LP_{02} and E_{13}-LP_{21b} modes, respectively. The E_{31}-E_{13} mode converter can be reduced from the previous three-stage linear taper of 12000 µm to approximately 4000 µm in length. Similarly, the E_{31}-LP_{02}, E_{13}-LP_{21b} mode converter can be reduced from the previous two-stage linear taper of over 6000 µm to approximately 4000 µm in length.

Keywords: mode converter, space division multiplexing, mode division multiplexing

Classification: Optical hardware

1. Introduction

With the rapid increase in Internet traffic, the demand for communication capacity expansion of optical fiber is increasing [1]. Since the 1980s, optical fiber communication technology has experienced several technical innovations, and the development of multiplexing technologies such as wavelength division multiplexing (WDM), time division multiplexing (TDM), and polarization division multiplexing (PDM) have increased the communication capacity of single-mode fiber. However, the communication capacity of conventional optical fiber is approaching its limit. In order to further expand the communication capacity, mode division multiplexing (MDM) transmission, which is one of the spatial division multiplexing (SDM) technologies, has received attention [2]. MDM can further expand the transmission capacity by using multiple spatial modes propagating in one optical waveguide as transmission channels.

The mode multiplexers (MUXs) or demultiplexers (DMUXs) are used to connect single-mode and multi-mode systems to realize the combination or separation of spatial modes in the MDM system. At present, on-board mode MUXs are primarily composed of Si waveguides [3, 4, 5, 6], polymer materials [7, 8, 9], and SiO_2-based planar lightwave circuits (PLC) [10, 11, 12, 13, 14, 15, 16]. This study focused on the SiO_2-based PLC which has advantages such as low loss and easy connection with optical fibers [12]. In the past few years, we have proposed two types of 6-mode MUXs based on asymmetric directional coupler (ADC) structures and photonic lantern (PL) structures, respectively [12, 16]. In the ADC-based 6-mode MUX, to achieve 6-mode multiplexing, a linear taper waveguide structure is utilized to realize the conversion from the E_{31} mode to the E_{13} mode, enabling the excitation of the E_{13} mode [12]. And in the 6-mode MUX based on PL, the output waveguide is rectangular in shape (which means that waveguide width W and waveguide height H are not equal), resulting in waveguide modes being emitted [16]. To facilitate better connectivity with optical fibers, it is necessary to convert the waveguide modes into fiber-like waveguide modes as shown in Fig. 1. This can be achieved by using a taper waveguide structure to transition from a rectangular waveguide ($W \neq H$) to a square waveguide ($W = H$) [17].

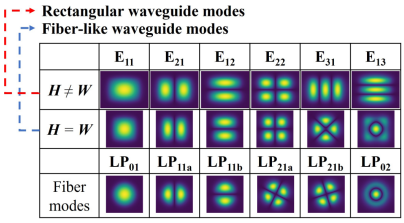

Fig. 1 Corresponding relationship between rectangular waveguide modes and optical fiber modes.

The previous PLC E_{31} and E_{13} mode converters used linear taper structures to fulfill the adiabatic coupling condition and achieve a high mode conversion efficiency, which requires long taper lengths. In recent years, a quantum-mechanics-inspired technique known as shortcut to adiabaticity (STA) [18, 19], has been increasingly applied in the field of optics [20, 21]. Recently, a novel STA protocol called fast quasiadiabatic dynamics (FAQUAD) has been proposed [22]. This method aims to accelerate the adiabatic coupling process by controlling the adiabatic parameters to achieve a uniform distribution during the coupling process. Devices such as Y-branch waveguides [26, 27, 28] and ADCs [23, 24, 25] designed using the FAQUAD approach have been reported. These devices achieve adiabatic coupling even with relatively short device lengths. However, current research on the FAQUAD protocol is primarily limited to the design of Si and polymer platforms. Although the SiO_2-based PLC mode converter for E_{12} and E_{21} modes has been proposed [29], only the 2LP mode operation is considered

[1] Graduate School of Information Science and Technology, Hokkaido University, Japan
[2] NTT Access Network Service Systems Laboratories, NTT Corporation, Japan
[a)] wang@icp.ist.hokudai.ac.jp

DOI: 10.1587/elex.20.20230392
Received August 22, 2023
Accepted October 13, 2023
Publicized October 23, 2023
Copyedited December 10, 2023

Copyright © 2023 The Institute of Electronics, Information and Communication Engineers

with complicated structures, and higher order modes have not been investigated.

In this paper, we propose two types of PLC taper structures that can be applied in different scenarios using FAQUAD. These structures enable mode conversions of E_{31}-E_{13}, as well as E_{31}-LP_{02} and E_{13}-LP_{21b}, respectively. Compared to the conventional linear structures, the proposed designs significantly reduce the taper length. The E_{31}-E_{13} mode converter can be reduced from the previous three-stage linear taper of 12000 µm [12] to approximately 4000 µm in length. Similarly, the E_{31}-LP_{02}, E_{13}-LP_{21b} mode converter can be reduced from the previous two-stage linear taper of over 6000 µm [12] to approximately 4000 µm in length.

2. Operation principle and device design

2.1 E_{31}-E_{13} mode converter

In this study, we used PLC waveguides with SiO_2 cladding, and the refractive index of the cladding is assumed to be 1.444. The relative refractive index difference between core and cladding is 1.0%. According to references [12], we have fixed the height of the waveguide to $H = 10$ µm and will focus our discussion solely on the waveguide width, denoted as W. Figure 2(a) shows the calculated waveguide width dependency of the effective refractive index when $H = 10$ µm at the wavelength of 1.55 µm. In Fig. 2(b), we have presented a zoomed-in view of the region corresponding to W ranging from 8 µm to 12 µm, as shown in the region enclosed by the red dashed line in Fig. 2(a). From Fig. 2(b), it can be seen that we can use a taper waveguide structure with a width ranging from 9 µm to 11 µm to achieve E_{31}-E_{13} mode conversions. Previously, such taper waveguides were constructed using a linear taper or a multi-stage linear taper structure [12]. However, to achieve a gradual adiabatic coupling process, an extremely long taper length L was required, resulting in a significant increase in the device size.

The adiabatic mode conversion process in optical waveguide devices requires the following relationship.

$$c(z) \equiv \left| \frac{\iint \left[\mathbf{E}_m \times \frac{\partial}{\partial z} \mathbf{H}_n^* \right] \cdot \boldsymbol{i}_z dxdy}{\beta_m - \beta_n} \right| \ll 1. \qquad (1)$$

Here, $c(z)$ is called the adiabaticity parameter. $\mathbf{E}_m$ and $\mathbf{H}_n$ represent the electric field distribution of the mth eigenmode and the magnetic field distribution of the nth eigenmode of the waveguide, respectively. β_m and β_n represent the propagation constants of the mth and nth modes, respectively. In this case, the mth mode corresponds to the E_{13} ~ LP_{02} ~ E_{31} mode (cyan line), and the nth mode corresponds to the E_{31} ~ LP_{21b} ~ E_{13} mode (orange line) in Fig. 2(b).

Figure 3(a) shows the linear taper structure with input waveguide width $W_{in} = 9$ µm and output waveguide width $W_{out} = 11$ µm. The waveguide height is fixed to $H = 10$ µm. Figure 3(b) shows the adiabaticity parameter $c(z)$ for the E_{31} and E_{13} or these hybrid modes in the linear taper. (The top axis represents the width of the linear taper waveguide, while the bottom axis represents the position z normalized to the taper length L in the propagation direction.) From Fig. 3, we can observe that the $c(z)$ of the linear taper waveguide

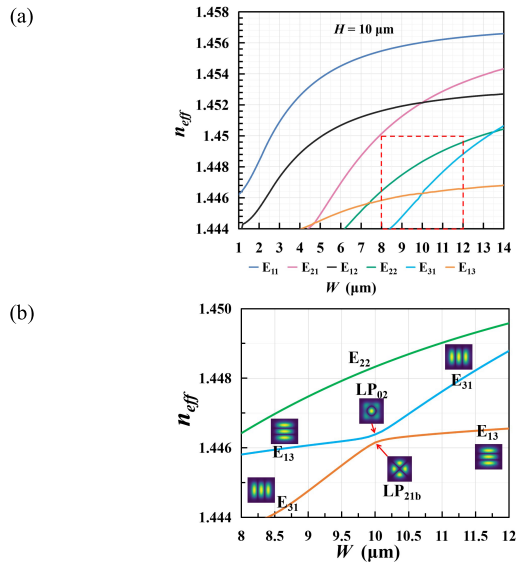

Fig. 2 (a) Waveguide width dependency of the effective refractive index when $H = 10$ µm. (b) The detail image of the region of $W = 8$~12 µm, as shown in the region enclosed by the red dashed line in Fig. 2(a).

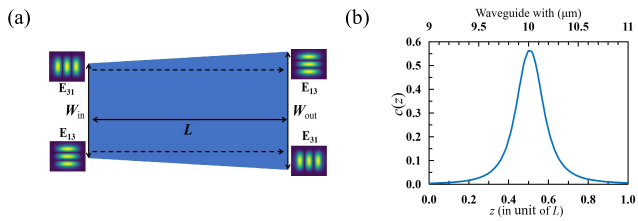

Fig. 3 (a) Linear taper structure with input waveguide width $W_{in} = 9$ µm and output waveguide width $W_{out} = 11$ µm. (b) The adiabaticity parameter $c(z)$ for the E_{31} and E_{13} or these hybrid modes in the linear taper waveguide from $W_{in} = 9$ µm to $W_{out} = 11$ µm.

sharply increases within the range of 9.5 µm to 10.5 µm in width. This implies that to satisfy the adiabatic coupling condition, the linear taper waveguide requires a sufficiently long waveguide length L to compensate for the large $c(z)$.

The FAQUAD method accelerates the adiabatic coupling evolution process by controlling the adiabatic parameters to achieve a uniform distribution during the adiabatic coupling process. The key to the FAQUAD method is to achieve a uniform distribution of the adiabatic parameter along the z-direction by fixing the adiabaticity parameter in Eq. (1) to a constant value ε. In other words, according to the following procedure [24], we should find $z_{opt}(W)$ satisfying $c(z) = \varepsilon$, where ε is a certain constant value. At the beginning, using the chain rule for z and W, Eq. (1) is rewritten as

$$c(z) = \left| \frac{dW}{dz} \right| \cdot c_W(W) = \varepsilon, \qquad (2)$$

$$c_W(W) = \left| \frac{\iint \left[\mathbf{E}_m \times \frac{\partial}{\partial W} \mathbf{H}_n^* \right] \cdot \boldsymbol{i}_z dxdy}{\beta_m - \beta_n} \right|. \qquad (3)$$

Since dW/dz is a constant in the linear taper waveguide, the adiabatic parameter for the linear taper waveguide as a function of W can be expressed as

$$c_{\mathrm{lin}}(W) = \frac{|W_{\mathrm{out}} - W_{\mathrm{in}}|}{L} c_W(W). \tag{4}$$

Substituting Eq. (2) into Eq. (4) and inverting z and W, we can obtain the following relationship.

$$\frac{dz}{dW} = \frac{L}{W_{\mathrm{out}} - W_{\mathrm{in}}} \cdot \frac{c_{\mathrm{lin}}(W)}{\varepsilon}, \tag{5}$$

noting that the sign of dz/dw should be coincident with that of $W_{\mathrm{out}} - W_{\mathrm{in}}$. Integrating Eq. (5) with the condition of $z(W_{\mathrm{in}}) = 0$, we can obtain $z_{\mathrm{opt}}(W)$ as

$$z_{\mathrm{opt}}(W) = \frac{L}{W_{\mathrm{out}} - W_{\mathrm{in}}} \frac{1}{\varepsilon} \int_{W_{\mathrm{in}}}^{W} c_{\mathrm{lin}}(t)dt, \tag{6}$$

where t is an integration variable. Noting that the length of the optimized taper given by z_{opt}, which is $L_{\mathrm{opt}} = z_{\mathrm{opt}}(W_{\mathrm{out}})$, depends on ε. If we fix ε to satisfy $L_{\mathrm{opt}} = L$, ε is derived as

$$\varepsilon = \frac{\int_{W_{\mathrm{in}}}^{W_{\mathrm{out}}} c_{\mathrm{lin}}(t)dt}{W_{\mathrm{out}} - W_{\mathrm{in}}}. \tag{7}$$

Substituting Eq. (7) into Eq. (6), we can finally obtain the structure of the FAQUAD taper waveguide with the taper length of L as the following expression.

$$z_{\mathrm{opt}}(W) = L \frac{\int_{W_{\mathrm{in}}}^{W} c_{\mathrm{lin}}(t)dt}{\int_{W_{\mathrm{in}}}^{W_{\mathrm{out}}} c_{\mathrm{lin}}(t)dt}. \tag{8}$$

By achieving a uniform distribution of $c(z)$ across the entire device, the length of the stronger coupling region can be adjusted to satisfy the adiabatic coupling condition, while the length of the weaker coupling region is minimized, thereby the length of the adiabatic taper waveguide can be greatly reduced. Figure 4(a) shows the shape parameters $z_{\mathrm{opt}}(W)$ of the linear and FAQUAD taper waveguides with waveguide widths ranging from $W_{\mathrm{in}} = 9\,\mu\mathrm{m}$ to $W_{\mathrm{out}} = 11\,\mu\mathrm{m}$. Figure 4(b) shows the structure of the FAQUAD taper obtained using the shape parameters from Fig. 4(a). Figure 5 shows the adiabaticity parameter $c(z)$ of the ideal FAQUAD taper using Eq. (7) (black dashed line), linear taper (blue line), and shape designed FAQUAD taper waveguide (structure in Fig. 4(b)) using Eq. (1) (red line). From Fig. 5, the adiabaticity parameter of the FAQUAD taper waveguide approaches that of the ideal FAQUAD design.

Since the waveguide shape parameters have been determined, the next step is to optimize the waveguide length by scanning the taper length L. Here, we use two calculation methods, BPM (Beam Propagation Method) and CLMT (Coupled Local Mode Theory), for the optimization of L. CLMT is a computationally accurate method for analyzing waveguide structures with varying widths. Figure 6 shows the approximated structure of a FAQUAD taper used in CLMT, which approximates the analytical structure as a continuous cuboid interval of length Δz. The field distribution at any arbitrary propagation position is approximated using the mode of the XY cross-section at the corresponding interval center $z = z_c$. The local coupled-mode equations

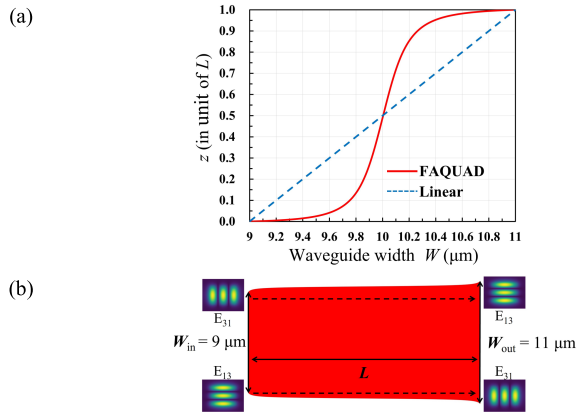

Fig. 4 (a) Shape parameters $z(W)$ for the linear and FAQUAD taper waveguides with waveguide widths ranging from $W_{in} = 9\,\mu\mathrm{m}$ to $W_{out} = 11\,\mu\mathrm{m}$. (b) The structure of FAQUAD taper obtained using the shape parameters from Fig. 4(a).

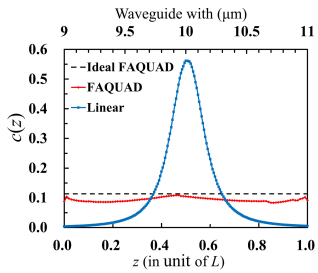

Fig. 5 Adiabaticity parameter $c(z)$ for the linear taper (blue line), ideal FAQUAD taper (black dashed line), and shape designed FAQUAD taper waveguide (red line).

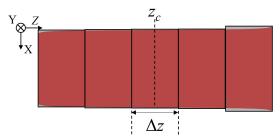

Fig. 6 Approximated structure of a FAQUAD taper used in CLMT.

of CLMT are expressed as follows [30].

$$\frac{da_m}{dz} = -\kappa_{mn}(z) \exp\left\{ j \int_0^z [\beta_m(z) - \beta_n(z)]\, dz \right\} a_n \tag{9}$$

$$\kappa_{mn}(z) = \iint \left[\mathbf{E}_m \times \frac{\partial}{\partial z} \mathbf{H}_n^* \right] \cdot \boldsymbol{i}_z dxdy \tag{10}$$

Here, a_m, a_n are the complex amplitude coefficients of the mth and nth modes, respectively. And κ_{mn} represents the coupling coefficient between the mth and nth modes.

Figures 7(a) and (b) show the relationship between the transmission for the input E_{31} mode and the waveguide length L in the case of (a) linear taper and (b) FAQUAD taper, when $W_{\mathrm{in}} = 9\,\mu\mathrm{m}$ and $W_{\mathrm{out}} = 11\,\mu\mathrm{m}$, respectively. From Fig. 7, it can be seen that the results of CLMT are basically consistent with those of BPM. According to the CLMT results, it is determined that a linear taper requires an L of 14200 μm to achieve a transmission over 90%, while an L of 30000 μm is needed to achieve a transmission over 99%. The FAQUAD taper only needs a length of about 4000 μm to achieve a transmission of over 99%. Figure 8

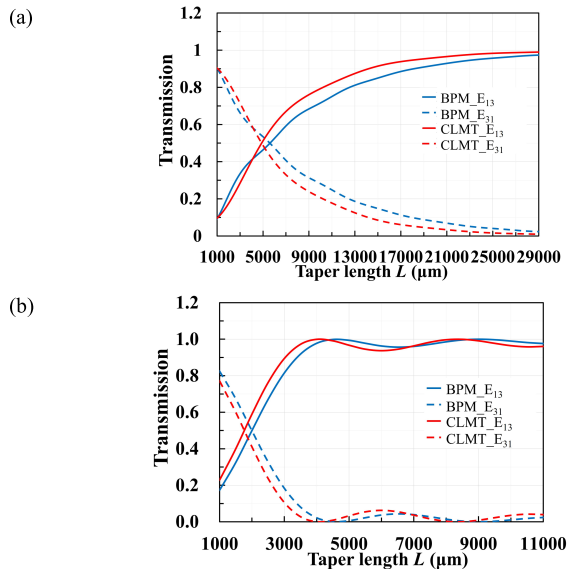

Fig. 7 Relationship between the transmission for the input E_{31} mode and L in the case of (a) linear taper and (b) FAQUAD taper, when W_{in} = 9 μm and W_{out} = 11 μm.

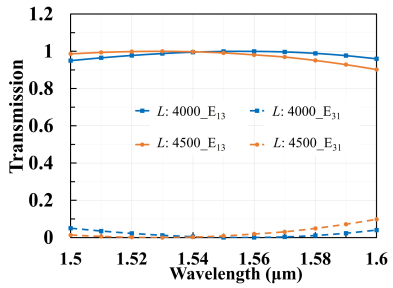

Fig. 8 Relationship between the transmission for the input E_{31} mode and the wavelength for FAQUAD E_{31}-E_{13} mode converter at various waveguide lengths.

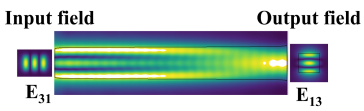

Fig. 9 The field distribution when E_{31} mode is input from the input port. The taper length L = 4000 μm, at the wavelength of 1.55 μm.

shows the relationship between the transmission for the input E_{31} mode and the wavelength of the FAQUAD E_{31}-E_{13} mode converter at various waveguide lengths (calculated by CLMT). According to Fig. 8, when L = 4000 μm or L = 4500 μm, the device can maintain transmission of over 90% within the wavelength range of 1.5 μm to 1.6 μm. Figure 9 shows the field distribution of the E_{31} mode input when L = 4000 μm, at the wavelength of 1.55 μm, which proves that the device can realize the E_{31}-E_{13} mode conversion with a shorter waveguide length.

2.2 E_{31}-LP_{02}, E_{13}-LP_{21b} mode converter

In the 6-mode MUX based on PL, the output waveguide is rectangular in shape, resulting in waveguide modes being emitted. To facilitate better connectivity with optical fibers, a tapered waveguide structure is needed at the output port to convert the rectangular waveguide into a square waveguide [17]. This enables the conversion of waveguide modes E_{31}

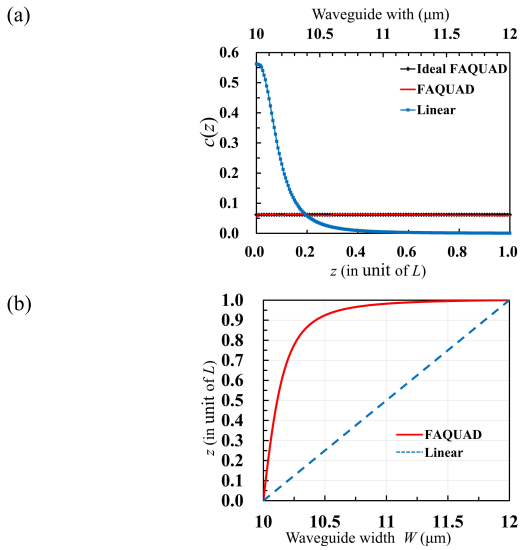

Fig. 10 (a) Adiabaticity parameter $c(z)$ for the linear taper (blue line), ideal FAQUAD taper (black line), and shape designed FAQUAD taper waveguide (red line). (b) Shape parameters $z(W)$ for the linear and FAQUAD taper waveguides with waveguide widths ranging from W_{in} = 12 μm to W_{out} = 10 μm.

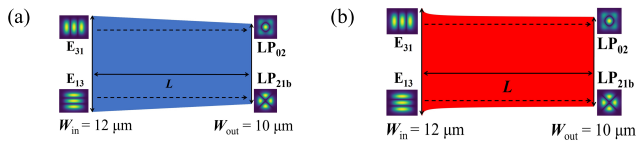

Fig. 11 (a) The structure of the linear E-LP taper. (b) The structure of the FAQUAD E-LP taper.

and E_{13} to fiber-like modes LP_{02} and LP_{21b}, respectively. To connect with the PL 6-mode MUX, we set the waveguide width at the input port of the mode converter to W_{in} = 12 μm, with the waveguide height fixed at H = 10 μm [16]. As mentioned in the previous section and indicated in Fig. 2(b), the E_{31}-LP_{02}, E_{13}-LP_{21b} mode converter (hereafter referred to as E-LP taper) can be achieved through a taper waveguide with the waveguide width from W_{in} = 12 μm at the input port to W_{out} = 10 μm at the output port.

Figure 10(a) shows the adiabatic parameter $c(z)$ of the ideal FAQUAD taper using Eq. (7) (black line), linear taper (blue line), and shape designed FAQUAD taper waveguide (structure in Fig. 11(b)) using Eq. (1) (red line). Figure 10(b) shows the shape parameters $z(W)$ of the linear and the FAQUAD E-LP taper with waveguide widths ranging from W_{in} = 12 μm to W_{out} = 10 μm. Figures 11(a) and (b) show the structure of the linear E-LP taper and the FAQUAD E-LP taper, respectively.

Figures 12(a) and (b) show the relationship between the transmission for the input E_{31} mode and the waveguide length L in the case of (a) linear E-LP taper and (b) FAQUAD E-LP taper, when W_{in} = 12 μm and W_{out} = 10 μm, respectively. From Fig. 12, it can be seen that the results of CLMT are basically consistent with those of BPM. According to the CLMT results, it is determined that a linear taper requires an L of 18000 μm to achieve a transmission over 90%, while over 50000 μm is needed to achieve a transmission over 99%. The FAQUAD taper only needs a length of about 4000 μm to achieve a transmission of over 99%. Figure 13 shows

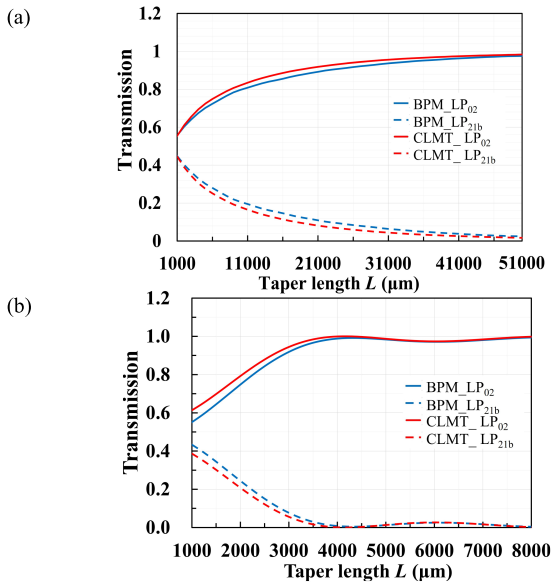

Fig. 12 Relationship between the transmission for the input E_{31} mode and L for the case of (a) linear E-LP taper and (b) FAQUAD E-LP taper, with W_{in} = 12 μm and W_{out} = 10 μm.

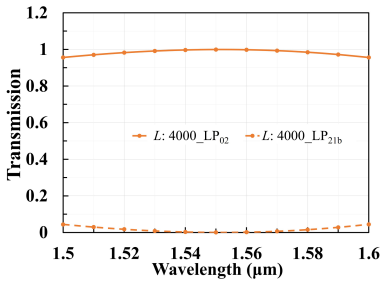

Fig. 13 Relationship between the transmission for the input E_{31} mode and the wavelength for FAQUAD E_{31}-LP_{02}, and E_{13}-LP_{21b} mode converter at various waveguide lengths.

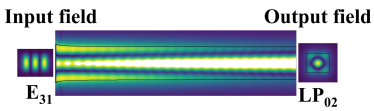

Fig. 14 The field distribution when E_{31} mode is input from the input port. The taper length L = 4000 μm, at the wavelength of 1.55 μm.

the relationship between the transmission for the input E_{31} mode and the wavelength of the FAQUAD E_{31}-LP_{02}, and E_{13}-LP_{21b} mode converter when the waveguide length is L = 4000 μm (calculated by CLMT). According to Fig. 13, when L = 4000 μm, the device can maintain transmission of over 95% within the wavelength range of 1.5 μm to 1.6 μm. Figure 14 shows the field distribution of the E_{31} mode input when L = 4000 μm, at the wavelength of 1.55 μm, which proves that the device can realize the E_{31}-LP_{02} mode conversion with a shorter waveguide length.

3. Conclusion

We proposed two types of PLC tapered structures that can be applied in different scenarios using FAQUAD. These structures enable mode conversions of E_{31}-E_{13}, as well as E_{31}-LP_{02} and E_{13}-LP_{21b}, respectively. In the case of the E_{31}-E_{13} mode converter, compared with the one-stage linear taper greater than 30000 μm, and the previous three-stage linear taper of greater than 12000 μm [12], the FAQUAD taper can achieve a transmission over 99% with a length of 4000 μm. In the case of the E_{31}-LP_{02}, and E_{13}-LP_{21b} mode converter, compared with the one-stage linear taper greater than 50000 μm, and the previous two-stage linear taper of greater than 6000 μm [12], the FAQUAD taper can achieve a transmission over 99% with a length of 4000 μm.

Acknowledgments

This work was supported by JST SPRING, Grant Number JPMJSP2119.

References

[1] T. Morioka: "New generation optical infrastructure technologies: 'EXAT initiative' towards 2020 and beyond," Optoelectron. Commun. Conf. (OECC) (2009) 1 (DOI: 10.1109/OECC.2009.5213198).
[2] T. Morioka, *et al.*: "Enhancing optical communications with brand new fibers," IEEE Commun. Mag. **50** (2012) 31 (DOI: 10.1109/MCOM.2012.6146483).
[3] W. Chang, *et al.*: "Ultra-compact mode (de)multiplexer based on subwavelength asymmetric Y-junction," Opt. Express **26** (2018) 8162 (DOI: 10.1364/OE.26.008162).
[4] Y. He, *et al.*: "Silicon high-order mode (de)multiplexer on single polarization," J. Lightw. Technol. **36** (2018) 5746 (DOI: 10.1109/JLT.2018.2878529).
[5] Y. Sawada, *et al.*: "Broadband and compact silicon mode converter designed using a wavefront matching method," Opt. Express **28** (2020) 38196 (DOI: 10.1364/oe.411769).
[6] W. Jiang, *et al.*: "Broadband mode (de)multiplexer formed with phase-matching of multimode access-waveguide," IEEE Photon. Technol. Lett. **33** (2021) 415 (DOI: 10.1109/LPT.2021.3067336).
[7] J. Dong, *et al.*: "Compact three-dimensional polymer waveguide mode multiplexer," J. Lightw. Technol. **33** (2015) 4580 (DOI: 10.1109/JLT.2015.2478961).
[8] Q. Huang, *et al.*: "Mode multiplexer with cascaded vertical asymmetric waveguide directional couplers," J. Lightw. Technol. **36** (2018) 2903 (DOI: 10.1109/JLT.2018.2829143).
[9] Q. Huang, *et al.*: "Six-mode multiplexer with cascaded vertical asymmetric waveguide directional couplers," Asia Communications and Photonics Conference (ACP) (2017) 1 (DOI: 10.1364/ACPC.2017.Su3K.5).
[10] N. Hanzawa, *et al.*: "Two-mode PLC-based mode multi/demultiplexer for mode and wavelength division multiplexed transmission," Opt. Express **21** (2013) 25752 (DOI: 10.1364/oe.21.025752).
[11] N. Hanzawa, *et al.*: "PLC-based four-mode multi/demultiplexer with LP_{11} mode rotator on one chip," J. Lightw. Technol. **33** (2015) 1161 (DOI: 10.1109/JLT.2014.2378281).
[12] K. Saitoh, *et al.*: "PLC-based mode multi/demultiplexers for mode division multiplexing," Opt. Fiber Technol. **35** (2017) 80 (DOI: 10.1016/j.yofte.2016.08.002).
[13] Y. Yamashita, *et al.*: "Design and fabrication of broadband PLC-based two-mode multi/demultiplexer using a wavefront matching method," J. Lightw. Technol. **35** (2017) 2252 (DOI: 10.1109/JLT.2016.2641461).
[14] T. Fujisawa, *et al.*: "Scrambling-type three-mode PLC multiplexer based on cascaded Y-branch waveguide with integrated mode rotator," J. Lightw. Technol. **36** (2018) 1985 (DOI: 10.1109/JLT.2018.2798619).
[15] M. Shirata, *et al.*: "Design of small mode-dependent-loss scrambling-type mode (de)multiplexer based on PLC," Opt. Express **28** (2020) 9653 (DOI: 10.1364/oe.387890).
[16] H. Wang, *et al.*: "6-mode and 10-mode photonic lantern mode multi/demultiplexers based on silica planar lightwave circuit," Opt. Commun. **529** (2023) 129098 (DOI: 10.1016/j.optcom.2022.129098).
[17] Y. Yamashita, *et al.*: "Excitation of LP21b and LP02 modes with

PLC-based tapered waveguide for mode-division multiplexing," Optoelectron. Commun. Conf. (OECC) (2016) 31.

[18] E. Torrontegui, *et al.*: "Shortcuts to adiabaticity," Adv. At. Mol. Opt. Phys. **62** (2019) 117 (DOI: 10.1016/B978-0-12-408090-4.00002-5).

[19] D. Guéry-Odelin, *et al.*: "Shortcuts to adiabaticity: Concepts, methods, and applications," Rev. Mod. Phys. **91** (2019) 045001 (DOI: 10.1103/RevModPhys.91.045001).

[20] T.-Y. Lin, *et al.*: "Mode conversion using optical analogy of shortcut to adiabatic passage in engineered multimode waveguides," Opt. Express **20** (2012) 24085 (DOI: 10.1364/OE.20.024085).

[21] D. Guo and T. Chu: "Silicon mode (de)multiplexers with parameters optimized using shortcuts to adiabaticity," Opt. Express **25** (2017) 9160 (DOI: 10.1364/OE.25.009160).

[22] S. Martínez-Garaot, *et al.*: "Fast quasiadiabatic dynamics," Phys. Rev. A **92** (2015) 043406 (DOI: 10.1103/PhysRevA.92.043406).

[23] H.-C. Chung, *et al.*: "Short and broadband silicon asymmetric Y-junction two-mode (de)multiplexer using fast quasiadiabatic dynamics," Opt. Express **25** (2017) 13626 (DOI: 10.1364/oe.25.013626).

[24] H.-C. Chung and S.-Y. Tseng: "Ultrashort and broadband silicon polarization splitter-rotator using fast quasiadiabatic dynamics," Opt. Express **26** (2018) 9655 (DOI: 10.1364/oe.26.009655).

[25] H.C. Chung, *et al.*: "Shortcuts to adiabaticity in optical waveguides," Epl. **127** (2019) 159 (DOI: 10.1209/0295-5075/127/34001).

[26] H.-C. Chung, *et al.*: "Compact polarization-independent quasi-adiabatic 2×2 3 dB coupler on silicon," Opt. Express **30** (2022) 995 (DOI: 10.1364/oe.446492).

[27] Y.-L. Wu, *et al.*: "Adiabaticity engineering in optical waveguides," Opt. Express **28** (2020) 30117 (DOI: 10.1364/oe.402545).

[28] Y.-J. Hung, *et al.*: "Mode-evolution-based silicon-on-insulator 3 dB coupler using fast quasiadiabatic dynamics," Opt. Lett. **44** (2019) 815 (DOI: 10.1364/ol.44.000815).

[29] T. Sato, *et al.*: "Design of silica-PLC LP_{11} mode rotator based on adiabatic mode conversion," Opt. Express **31** (2023) 23910 (DOI: 10.1364/OE.493501).

[30] D.F. Siriani and J.-L. Tambasco: "Adiabatic guided wave optics — a toolbox of generalized design and optimization methods," Opt. Express **29** (2021) 3243 (DOI: 10.1364/oe.415653).